Level-Crossing Spectroscopy in 7 ^2S Thallium. I. Studies of Coherence-Narrowing, Collision-Broadening, and Buffer-Gas Effects*

J. C. Hsieh†
Department of Chemistry, Brown University, Providence, Rhode Island 02912
and
J. C. Baird‡
Joint Institute for Laboratory Astrophysics, University of Colorado, Boulder, Colorado 80302
(Received 23 August 1971)

The lifetime, coherence narrowing, and collision broadening of the $7\,^2S_{1/2}$ excited state of atomic thallium has been studied by the technique of zero-field level-crossing spectroscopy. The lifetime of the $7\,^2S_{1/2}$ state is determined to be 7.55(0.08) nsec. The full coherence-narrowing effect gave a branching ratio, from $F=1$ of $7\,^2S_{1/2}$ to the ground state, of 43%. The cross section for thallium-thallium resonance-broadening collisions is $\sigma_{\mathrm{Tl-Tl}}=5.38(0.49)\times 10^{-8}/\bar{v}$ cm^2. The effect of 426-torr helium on the thallium lifetime, coherence narrowing, and resonance broadening was also investigated. From the low-thallium-density region the cross section for helium depolarization of the thallium $7\,^2S$ state is $\sigma_{\mathrm{Tl-He}}\cong 7\times 10^{-13}/\bar{v}$ cm^2. There is also indication of a buildup of population in the metastable $6\,^2P_{3/2}$ thallium state. From the data, the cross section for the process $\mathrm{Tl}(6\,^2P_{3/2})\rightarrow \mathrm{Tl}(6\,^2P_{1/2})$ by helium collisions is $\sigma\simeq 1\times 10^{-21}$ cm^2. The Tl branching ratio in the presence of helium is 39%. It was also found that the thallium-thallium resonance-broadening cross section is $\sigma_{\mathrm{Tl-Tl}}=4.04$ (0.32) $\times 10^{-8}/\bar{v}$ cm^2 in the presence of 426 torr of helium. In the presence of 113 torr of He, the resonance-broadening cross section was found to be $\sigma_{\mathrm{Tl-Tl}}=5.22$ (0.13) $\times 10^{-8}/\bar{v}$ cm^2. In the case of Ar as the buffer gas, $\sigma_{\mathrm{Tl-Ar}}=8\times 10^{-13}/\bar{v}$ cm^2.

I. INTRODUCTION

Resonance fluorescence in atomic thallium under level-crossing conditions leads to the observation of several physical effects: the free decay of excited atoms; radiation-trapping coherence narrowing; and depolarization of resonance radiation by collisions. In this paper we report on level-crossing studies with thallium and with thallium in the presence of helium and argon.

Because there are two well-separated fine-structure branching states (see Fig. 1) in the atomic thallium ground state, 3776-Å resonance radiation can be used for excitation and 5350-Å scattered cross-fluorescence radiation can be used for detection of the level crossing between the $F=1$, $|M_F|=1$, and $M_F=0$ levels of $7\,^2S_{1/2}$. This avoids severe depolarization of the detected photons since the system may become optically thick for 3776-Å photons while it is nearly always optically thin for the 5350-Å photons. The experiment may therefore be carried out from low atom densities, $\sim 10^{10}$ atoms/cm^3, to relatively high densities 2×10^{15} atoms/cm^3, and into the collision broadening region.

In the experiment, the linewidth is observed independently of the Doppler effect. Thus, at low atomic-thallium densities, the decay of essentially free atoms leads to a measurement of the excited-state natural lifetime.[1] As the atomic density is increased there is an evolution to a loose many-body system in which a coherence narrowing of the excited-state levels occurs (one form of radiation trapping); and finally, owing to the dominance of the large resonance-collision cross section betwee thallium atoms, there is a collision-broadening contribution to the linewidth. The addition of a foreign buffer gas provides the opportunity of observing competing processes between the gas and thallium. At low thallium-atom densities and a

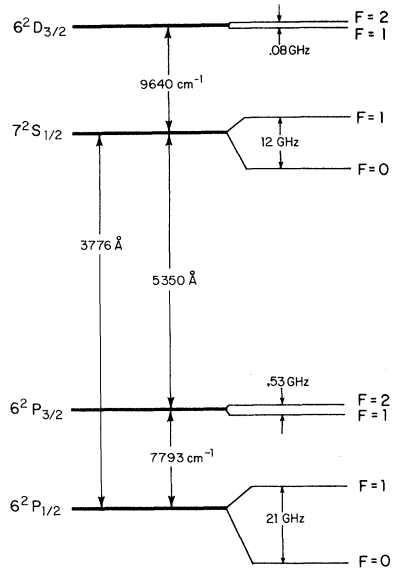

FIG. 1. Energy levels and their separations of interest in thallium.

constant buffer-gas density there is both the process of independent thallium-atom decay and buffer-gas collisional depolarization of thallium. This increases the width of the level-crossing signal from the thallium excited state and yields a measurement of the cross section for the process. At higher Tl densities, $\sim 10^{12}$ atoms/cm^3, the helium collisions interfere with the coherence-narrowing process. This arises in two ways: (a) The presence of helium removes an important relaxation process (wall collisions) which maintains thermal equilibrium between the two fine-structure states of the ^2P multiplet in thallium, thus allowing another channel for radiation trapping. (b) The presence of helium apparently alters the branching ratio of the thallium transition. Finally, as the resonance-collision process dominates, it is observed that, in the presence of helium, the apparent cross section for thallium deexcitation by thallium is reduced.

Systematic studies using the level-crossing technique, besides those of measuring lifetimes and g factors, are limited. The only complete study of the lifetime, coherence narrowing, and resonance broadening was made by Saloman and Happer on the $^3P_1$ state of lead.[2,3] However, the effect of rare-gas atoms on the coherence narrowing and resonance broadening processes has not been studied previously. At present, both the theory and experimental data are for atoms in vacuo. In our experimental work, we first explore the interaction of free thallium atoms. Later we extend the technique to thallium atoms in the presence of helium and argon.

II. THEORY

A. Level-Crossing Signal Line Shape

It has been a standard procedure to derive the expression for the level-crossing signal line shape starting from the so-called Breit equation.[4,5] In the case of the thallium $7\,^2S_{1/2}$ state, having $J=\frac{1}{2}$, the derivation by Rose and Carovillano turns out to be clearer for the deduction of selection rules.[6] The detailed calculation of the selection rules is presented in the Appendix. In order to obtain a level-crossing signal, in the present experiment, both the incident and detected light beams must be circularly polarized. In the notation of the Appendix, only the $\nu=1$, $|\mu-\mu'|=1$ level-crossing signal is allowed. For our experimental setup, 3776-Å incident light is used and 5350-Å scattered light is detected. The signal expression is taken to be

$$S = A - B\frac{(\pm)(\pm)\sin\theta_1\sin\theta_2}{1+(E_{\mu\mu'}\tau)^2} \times [\cos(\phi_1-\phi_2)+E_{\mu\mu'}\tau\sin(\phi_1-\phi_2)], \quad (1)$$

where the constants A, B are for the incoherent part and the coherent part of the signal, respectively; $(\pm)$ refers to the sense of circular polarization of the incident and detected light beams, e.g., (+) for right-circular polarization and (−) for left; $E_{\mu\mu'}$ is the energy separation between the two excited-state crossing sublevels μ, μ'; τ is the mean lifetime of the excited state; θ_1, ϕ_1 are the polar and azimuthal angles of the incident light beam; and θ_2, ϕ_2 are corresponding angles for the detected light beam.

Equation (1) is equivalent to Eq. (13) from Gallagher and Lurio, Ref. 7, except that (i) the magnitude of the coherent part of the expression is different. [This is because Eq. (13) of Ref. 7 was derived by assuming scattered 3776-Å light was detected, instead of 5350-Å light, and so the values of the phase factor in Eq. (A4) are different.] (ii) The magnitude of the coherent part of the signal B is smaller than the value in Eq. (13) of Ref. 7 because the values of the J_2-dependent $6j$ symbol in the M_2-matrix element [cf., Eq. (A4)] are different in the two cases.

When θ_1, $\theta_2=\pm 90°$ and $(\phi_1-\phi_2)=\pm 180°$, Eq. (1) reduces to the usual Lorentzian signal result. Similarly, when θ_1, $\theta_2=\pm 90°$, and $(\phi_1-\phi_2)=\pm 90°$, Eq. (1) reduces to the dispersion-shaped signal expression.

Since $E_{\mu,\mu'}=g_F\mu_B(\mu-\mu')H/\hbar=g_F\mu_B H/\hbar$ and $g_F=1$, the lifetime τ is obtained in the form

$$\tau = 2\hbar/\mu_B H_{1/2},$$

where μ_B is the Bohr magneton, g_F is the g factor of the excited state, H is the magnetic field strength in gauss, and $H_{1/2}$ is either the half-width of a Lorentzian signal or the peak-to-peak separation of a dispersion signal.

B. Coherence Narrowing

If the atomic density in the resonance cell is low enough, only spontaneous emission is involved in the relaxation of the excited-state atoms, and the measured lifetime from a level-crossing signal would be the natural lifetime τ_0. But when the atomic concentration is increased, the photon mean free path of the resonance radiation is reduced. The probability that the emitted photons will be reabsorbed and reemitted at least once before leaving the cell boundary may become significant, and, as a result, the measured lifetime is increased. This repeated absorption and reemission process is called imprisonment of resonance radiation,[8] radiation trapping, or multiple scattering.[9] By the nature of the level-crossing experiment, in which the excitation and detection are coherent, the narrowing effect of the multiple scattering on the linewidth of the level-crossing signal is therefore called coherence narrowing.

Barrat[10] first systematically studied this coherence-narrowing effect. D'yakonov and Perel[11] improved Barrat's theory by taking the velocity distribution of the atoms into account and arrived at the

same physical result as Barrat, except that the reabsorption probability of the emitted photons has an integral form instead of a single exponential. Recently, Saloman and Happer[2,3] have extended Barrat's theory to include the case of branching decay. Branching decay means that the excited atoms can decay to more than two lower states. Their results showed

$$1/\tau_c^L = (1 - \textstyle\sum_i \alpha_i x_i \mathcal{B}_i)(1/\tau_c) \ , \tag{2}$$

where i refers to the ith branching state; $\mathcal{B}_i$ are the branching ratios; τ_c^L is the coherence time measured from the half-width of the level-crossing signal. The superscript L refers to the multipolarity of the emitted radiation. In this work, only $L = 1$ signals are detected and we therefore drop L as a superscript. α_i, which depends on the total initial and final angular momentum, is the depolarization factor. x_i, a function of density, is the reabsorption probability of emitted photons and can be expressed by[11]

$$x_i = 1 - \frac{1}{\sqrt{\pi}} \int_{-\infty}^{+\infty} \exp\left[-t^2 - \left(\frac{\pounds}{l_i} e^{-t^2}\right)\right] dt \ ,$$

$$l_i = \frac{2F_i + 1}{2F + 1} \frac{8\pi^{3/2} \bar{v} \tau_0}{N_i \lambda_i^3 \mathcal{B}_i} \ ,$$

where $\pounds$ is a characteristic cell length, l_i has the units of length and is equivalent to the mean free path of a photon in the center of the ith branching-decay line, F_i and F are the total angular momentum of the ith branching state and total initial angular momentum, respectively, and λ_i is the wavelength of the ith branching decay line.

The separation of the two hyperfine levels of the $6\,^2P_{1/2}$ thallium state is about 2.1×10^4 MHz and is well resolved with respect to the Doppler width. Thus, these two levels can be considered as two branching states and they will contribute to the coherence-narrowing and resonance-broadening effects independently, although they are not optically separated. Similarly, since the separation of the two hfs levels of the $7\,^2S_{1/2}$ thallium state is about 1.2×10^4 MHz, and is larger than the natural linewidth (1.3×10^2 MHz), there will be no crossing between the two hfs levels. In other words, the detected level-crossing signal originates from the $F = 1$ excited-state level only.

C. Collision Broadening

When the atomic density is increased, the interaction between a radiating atom and every other atom in the vapor may become significant. This atom-atom coupling may be approximated by the dipole-dipole interaction term. The matrix element of this interaction between the ground and excited states is nonzero for identical colliding atoms. Thus, if the transition has a large oscillator strength, as in this work, this matrix element will be relatively large, and eventually the excitation energy will be exchanged between the atoms. The corresponding resonance-broadening cross section will be much larger than typical kinetic cross sections.

The theory of resonance broadening (self-broadening in general), employing reasonable approximations, has been extensively worked out by various authors.[12–15] For the branching-decay mode, the result for the resonance-broadening part of the linewidth γ may be written as

$$\gamma = \textstyle\sum_i N_i \sigma_i \bar{v} \tag{3}$$

and

$$\sigma_i = C_i(\lambda_i^3 \mathcal{B}_i / \bar{v} \tau_0),$$

where i refers to the ith branching state, N_i are the atomic densities, σ_i are the resonance-broadening cross sections, and $\bar{v}$ is the relative velocity of the colliding particles; C_i is a constant whose value depends upon various collision-theory approximations made, the total angular momentum of the initial and final states, the wave functions of the initial and final states, and the multipolarity. It is obvious that γ is velocity independent. Consequently, a straight line will be obtained for γ vs N (thallium density). The over-all linewidth including spontaneous emission, coherence narrowing, and resonance broadening becomes

$$\Gamma = \Gamma_0 - \textstyle\sum_i \alpha_i x_i \mathcal{B}_i \Gamma_0 + \sum_j N_j \sigma_j \bar{v} \ , \tag{4}$$

where Γ is the over-all linewidth, Γ_0 is $1/\tau_0$, and the rest of the notation has been described previously.

III. EXPERIMENTAL RESULTS

In the experiment, we investigate the changes in linewidth as the atomic concentration is varied. Because the degree of linewidth change is small, e.g., in the case of coherence narrowing the maximum range of the effect is only 11% of the natural width, it was necessary to use digital data-handling techniques to process relatively large quantities of data and to optimize the apparatus in every respect in order to obtain the level-crossing signal shape and position with high accuracy. The experimental setup consists of a light source, lens system to produce a parallel beam of resonance radiation covering the cylindrical thallium cell, a filter passing 3776-Å radiation, a circular polarizer, a light pipe, an oven, a thallium cell, another light pipe along the cylindrical cell axis, another analyzer, a 5350-Å filter, and a lens to focus the 5350-Å light onto the photocathode of a photomultiplier. The output of the photomultiplier is fed to the digital signal-processing equipment. The thallium cell and oven are situated in the center of several sets of Helm-

holtz coils, one set supplying the level-crossing field perpendicular to the optical axis and two sets used to cancel the earth's field.

The light source is formed by a dc discharge in a commercial Osram thallium lamp. In order to stabilize the lamp output, a 63-Ω resistor (a commercial heating unit) was connected in series with the lamp. The resistor was cooled by running water. The dc power supply was a Kepco model SM-160-2A(M). This unit supplied about 80 W of power to the circuit, of which about 65 W were dissipated by the resistor. The lamp was initially excited by 220-ac obtained from a transformer. It was found that slight air turbulence, caused, for example, by movement near the lamp, produced an effect on the lamp output. Therefore, the space around the lamp was enclosed by a cloth. While data were being taken, the lamp output was monitored with a RCA 935 phototube and its output displayed on a 12-in. strip-chart recorder. The lamp noise level was always too small to be seen on the recorder, but it was estimated that the noise level was always $< 0.2\%$ (S/N of the lamp output was always several hundred). The lamp profile was estimated to be about ten times the absorption profile.

The thallium atoms were supplied by heating the cylindrical resonance cell which contained a small amount of thallium metal. The quartz resonance cells were first outgassed to a pressure of less than 10^{-6} torr for several days at a temperature between 750 and 950 °C. After outgassing, a few milligrams of spectrographic-grade thallium (Mahafy-Johnson), which had itself been outgassed, was distilled into the cell. Further cleaning was attempted by sparking the cell with a Tesla coil for a short period. At sealoff the pressure was always in the 10^{-7} range. The thallium resonance cells were 2.5 cm in diameter and 2.5 cm long. Both ends of the cell were sealed with quartz windows. The cell heating oven was composed of two Fischer semicylindrical heating units, 6.3-cm i.d. and 6.3 cm long, embedded in Alumdum cement. The ac heating current was found to have no effect on the signal linewidth and line shape. The heating wire was nonferromagnetic and was wound in a helix. To improve the thermal uniformity around the cell, a piece of copper bushing served as a heat sink. The whole assembly (oven, bushing, and cell) was placed inside a $15 \times 15 \times 16$ cm refractory housing. With this setup, a temperature difference of 10.9 °C was found between the center of the cell window and the center of the cylindrical body of the cell. This temperature difference was found to be maintained throughout the 350–750 °C temperature range of the experiment.

For resonance cells containing both thallium and a buffer gas the following procedure was followed. A liter flask of spectroscopic-grade helium (Airco), or argon, was previously attached through a valve to the vacuum system as was a mercury manometer. After outgassing and distillation of the thallium to the cell, as outlined above, a breakseal on the rare-gas flask was broken. The rare-gas pressure was monitored by a thermocouple gauge and after sealoff of the resonance cell the manometer was cut into the system and the rare-gas pressure more accurately measured.

The temperature was measured with a chromel-alumel thermocouple whose reference junction was maintained at 0 °C by an ice-water bath. The emf produced by the thermocouple was amplified by an operational amplifier, and the amplified voltage displayed on a digital voltmeter (DVM). The DVM is actually composed of a Hewlett-Packard 5245 eight-digit electronic counter with a 5265 analog-to-digital converter plugin. A RFL model 70 temperature controller which has an accuracy of 0.05 °C was used to control the temperature of the cell.

The magnetic field was produced by a pair of 16-in.-i.d. Helmholtz coils which were constructed from wire wound onto a 2-in. aluminum channel. The stepwise sweeping of the magnetic field was achieved by switching the position of a set of resistors connected to the programming terminals of the power supply (NJE) model RVC 36-25. The magnetic field was determined by measuring the voltage drop across a 0.23-Ω resistor (henceforth called the standard resistor) which was connected in series with the Helmholtz coils. The resistor was constructed from constantan wire which has the lowest temperature coefficient of resistivity among the common metals and alloys.[16] The ratio of gauss vs voltage drop was determined using a modified Rawson-Lush No. 824 rotating-coil gaussmeter whose accuracy was better than 0.05 G. The mean value of this ratio was 13.391 (0.017) G/V with a standard deviation of about 0.15% over a 2-month period. This shows that both the resistance of the standard resistor and the gaussmeter were stable in time. In spite of the smallness of the earth's field, two pairs of large (36-in.) Helmholtz coils placed perpendicular to each other were used to eliminate the components of the earth's field.

The analyzer for the incoming light consisted of a 3776-Å interference filter, a polaroid uv linear polarizer, and a quarter-wave plate for 3776-Å. The analyzer for the scattered light was made from either a 5350-Å filter, a linear polarizer and a 140-mμ polaroid retardation plate, or a polaroid HGCP 21 green circular polarizer. The incident and scattered light were axial to the cylindrical scattering cell. The detector was an 11-stage EMI 9524S photomultiplier. The tube was well shielded magnetically. The output of the photomultiplier was directly fed to the DVM.

The data were taken in the following sequence: After at least 12 h of warmup of all equipment, the

lamp was turned on. 1 h later, the oven heater was turned on and the temperature preset. After the lamp had reached a steady output intensity and the temperature at the cell had become stable, the temperature reading was punched onto paper tape. The magnetic field was then stepped from roughly +75 to −75 G in about 23 steps in different increments, smaller increments being taken nearer zero field. At each field point, the voltage drop across the standard resistor was punched onto paper tape at the beginning and the end of each step, and, in between, about ten values of the signal strength were also punched onto tape. The number of values of signal strength punched at each field point depended on the S/N ratio. At the end of each run, another temperature reading was punched to complete one run of data. Two runs were taken at each temperature. Following the procedure just described, a roll of paper tape which contained a long strip of data was obtained covering a given Tl atom-density range. Later the tape was read by an IBM 2671 paper-tape reader and data were fed to an IBM 360 computer for data processing and least-squares fitting. The linewidth and other results were obtained from the computer output.

IV. RESULTS AND DISCUSSION

A. Calculation of Thallium Density

If one is only interested in measuring the natural lifetime of an excited state from a level-crossing experiment, knowledge of the atomic concentration is not needed as long as the data are taken in the low-density region where there is no radiation trapping. This is the most promising advantage of the level-crossing technique for measuring the excited-state lifetime. But in this work, we are most interested in phenomena, such as coherence narrowing and resonance broadening, which are directly related to the atomic density as the second and third terms in Eq. (4) show. Thus in this experiment, accurate thallium-density measurements are required. The most accurate way of measuring atomic density, of course, is to directly measure the transmittance of some specific reference light. Since this method is very difficult, a practical way is to measure the temperature and then calculate the corresponding atomic density from available vapor-pressure data, providing they are reliable. In fact, this is the most common method used in level-crossing spectroscopy.

The most reliable source of thallium vapor pressure we believe is the data obtained by Genov *et al.*[17] That part of their data covering the entire density range used in this work can be fitted by the equation $\log_{10} P = A + B/T$, where T is the temperature in °K, P is the pressure in torr, and A, B are two parameters. A least-squares fit of the equation to the data gives $A = 8.0576$ and $B = -8868.4$. These fitted results[18] are almost identical to the data of Honig.[19]

B. Signal Processing

By using a digital-data acquisition and stepwise scanning of the magnetic field, the data can be easily analyzed by computer. The computer program[18] processes the data [which were punched on tape in binary-coded decimal (BCD) and then read by an IBM 2761 tape reader] converting them into decimal form and then calculating average values, and rms errors, of the magnetic field and signal strength at each field point. Later, these data are least-squares fitted to Eq. (1). The fitting process used a weighted nonlinear least-squares procedure.[20] Most of the figures shown in this work were plotted by computer (CALCOMP) to assure accuracy in drawing.

In this work, we mainly employ the experimental configuration by which a Lorentzian signal is detected, i.e., 3776-Å circularly polarized exciting light and 5350-Å scattered light detected through a circular polarizer. The directions of the two beams are both perpendicular to the direction of the magnetic field (θ_1, $\theta_2 = \pm 90°$) but separated by 180° ($\phi_1 - \phi_2 = 180°$).

Figure 2 shows a typical Lorentzian signal. The solid line is the result of a least-squares fit to Eq. (1). The agreement between experimental points and the theoretical line shape is very good over a range of five half-widths. The sign of the coherence part of the signal in Eq. (1) is justified by noticing the sense of the circular polarization in the incident and scattered light. Two strings of data points on the upper part of Fig. 2 indicate that no signals are detected when one or both of the exciting and scattered light beams are not circularly polarized. This confirms the selection rules which we deduce in the Appendix. These two strings of data may be considered as background signals. The slight curvature in them may be due to the lamp profile, resulting from a small amount of self-reversal, as well as a slight imperfection in the magnetic shielding of the photomultiplier. Since the irregularities in the background are quite small and random, we do not take the background into account in the linewidth analysis. The experimental results will be described in two parts: first, the case of pure-thallium level crossing, and second, the case of thallium level crossing in the presence of a rare gas.

C. Pure Thallium

Figure 3 shows the linewidths vs $\log_{10}$ thallium density from 10^{10} to 2×10^{15} atoms/cm^3, thus covering three different regions: spontaneous emission, coherence narrowing, and resonance collision broadening. The solid curve is the result of fitting

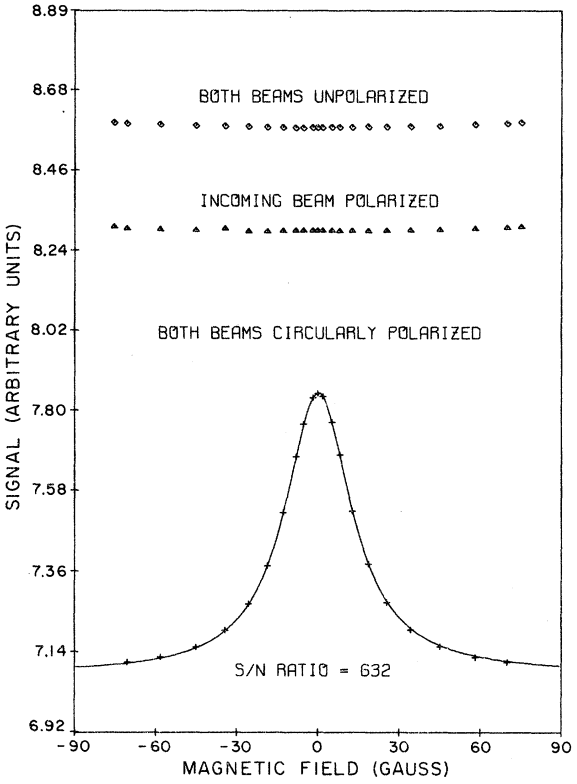

FIG. 2. Typical Lorentzian signal. The geometry is $(\phi_1-\phi_2)=\pi$, $\theta_1=\frac{1}{2}\pi$, $\theta_2=-\frac{1}{2}\pi$. The solid line is the result of a least-squares fit of the theoretical expression to the signal.

data to Eq. (4). In the fitting, the two hfs components of the ground state are considered as two branching states and only the $F=1$ level of the $7\,^2S_{1/2}$ state is considered as an excited state. Three parameters were assigned in the fitting, corresponding to the natural linewidth Γ_0, the branching ratio to the $F=0$ level of the ground state $\mathcal{R}_1$, and the thallium resonance-broadening cross section $\sigma_{Tl\text{-}Tl}$. The following approximations are made in fitting the data. (a) The branching ratio to the $F=1$ level of the ground state is assumed to be twice the value to the $F=0$ level, i.e., $\mathcal{R}_2=2\mathcal{R}_1$. This is based on the intensity ratio of the two hfs components. (b) The ground-state population is considered to be evenly distributed between the two hfs, because the hfs separation is extremely small compared to kT, with $T\sim 600\,^\circ$C. (c) The concentration of the $6\,^2P_{3/2}$ metastable state is neglected since the fs structure tion is far larger than kT and since the wall relaxation of the state is fast enough ($\sim 3\times10^{-5}$ sec) to suppress the buildup of the metastable-state concentration. This has previously been proved in lead.[2,3]

At low densities ($<6\times10^{10}$ atoms/cm^3), the linewidth remains essentially constant. This indicates that only spontaneous emission contributes to the linewidth. When the density gradually increases, the linewidth starts to decrease, indicating the onset of coherence narrowing. The linewidth then reaches a maximum narrowing region at about 4×10^{12} atoms/cm^3, where the reabsorption probability of the emitted photons, x_i, approaches unity. When the Tl density is further increased, the linewidth rapidly increases again, indicating that collision broadening is taking place. These linewidth characteristics fully agree with theory [Eq. (4)].

From the limiting linewidth at low densities, the first parameter in the fitting procedure is obtained: $\Gamma_0=1.325\ (0.015)\times10^8$ sec^{-1} or a natural lifetime for the $7\,^2S_{1/2}$ state of $\tau_0=7.55\ (0.08)\times10^{-9}$ sec. The uncertainty is calculated from the average error of the experimental points deviating from the fitted curve up to the maximum narrowing region. The value of τ_0 is in excellent agreement with the value $7.6\ (0.2)\times10^{-9}$ sec reported in Ref. 7 and the value $7.45\,(0.2)\times10^{-9}$ sec reported recently by Norton and Gallagher.[21]

The result of the fitting also gives $\mathcal{R}_1=1.880\times10^6/\Gamma_0$, the branching ratio to the $F=0$ level of $6\,^2P_{1/2}$ state. From the value of $\mathcal{R}_1$, Γ_0, and the hfs intensity ratios, the branching ratio to the $6\,^2P_{1/2}$ state is calculated to be 0.43. The ratio of the probabilities of the $F=1$, $7\,^2S_{1/2}-6\,^2P_{3/2}$ transition (5350 Å) to the $F=1$, $7\,^2S_{1/2}-6\,^2P_{1/2}$ transition (3776 Å) is calculated to be

$$\frac{A(5350\text{ Å})}{A(3776\text{ Å})}=\frac{1-\mathcal{R}}{\mathcal{R}}=1.33\ .$$

This value for the ratio of transition probabilities differs from that reported in Ref. 7 and may reflect the accuracy of the radiation-trapping theory as

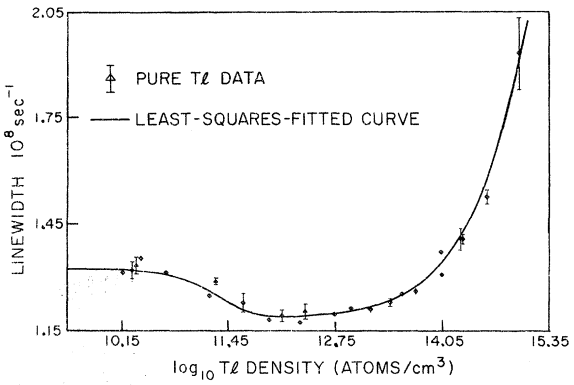

FIG. 3. Data for the pure-thallium case: Level-crossing signal as a function of thallium density covering three regions—spontaneous emission, coherence narrowing, and resonance broadening. The solid line is the result of a least-squares fit to Eq. (4).

applied to this experiment. For example, our experiment employs cylindrical geometry while the usual theories[12–15] assume spherical symmetry.

In Fig. 3, when the thallium density is greater than 10^{14} atoms/cm^3, the linewidth rapidly increases. The linewidths, taken at high thallium densities, are plotted in Fig. 4. The result of a weighted least-squares fit is a straight line with a slope of $5.38(0.17)\times10^{-8}$ cm^{3}sec^{-1}. From Eq. (4), it can be seen that this slope represents the product of the over-all resonance-broadening cross section $\sigma_{Tl\text{-}Tl}$ and the relative velocity $\bar{v}$. The cross section $\sigma_{Tl\text{-}Tl}$ is comprised of cross sections for the $F=0$ and $F=1$ states of $6\,^2P_{1/2}$. Therefore, we may write

$$\sigma_{Tl\text{-}Tl}\,\bar{v} = \tfrac{1}{4}(\sigma_1\bar{v} + 3\sigma_2\bar{v}) = 5.38\,(0.17)\times10^{-8}\ \text{cm}^3\,\text{sec}^{-1}$$

where the subscripts 1 and 2 refer to the $F=0$ and $F=1$ levels of the $6\,^2P_{1/2}$ state, respectively. The values of σ_1 and σ_2 cannot be measured separately because the $F=1$, $7\,^2S_{1/2}-F=0$, $6\,^2P_{1/2}$ and $F=1$, $7\,^2S_{1/2}-F=1$, $6\,^2P_{1/2}$ lines are not optically separated.

We estimate that the uncertainty in the experiment of Genov *et al.*,[17] measuring the thallium vapor-pressure–temperature relation is 6%. By taking this uncertainty into account, the thallium resonance-broadening cross section becomes $\sigma_{Tl\text{-}Tl}\bar{v} = 5.38\,(0.49)\times10^{-8}$ cm^{3}sec^{-1}. At 700 °C, $\bar{v}=4.5\times10^4$ cm sec^{-1}, and we obtain $\sigma_{Tl\text{-}Tl} = 1.20\,(0.11)\times10^{-12}$ cm^2 which is 10^4 times the gas-kinetic cross section. This fact, along with the good linearity between linewidth and density, implies that the broadening is resonant, as expected.

D. Thallium in Presence of Helium and Argon

Cells containing 113 and 426 torr of helium and 419 torr of argon in addition to thallium were prepared. Using these cells, data were gathered from low thallium densities and into the resonance-broadening region. The 113-torr cell showed results consistent with the higher-density helium cell, but not as pronounced and those data will not be discussed further.

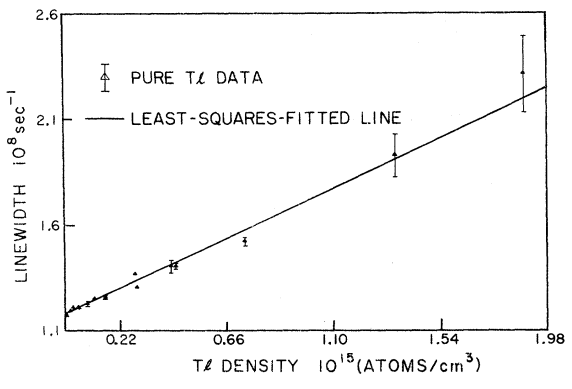

FIG. 4. Data for the pure-thallium case: Effect of thallium resonance broadening. The quoted error represents the error obtained from a least-squares fit, only it does not include the uncertainty for the density measurement.

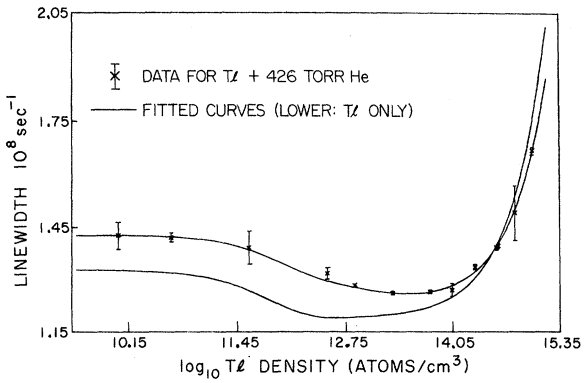

FIG. 5. Data for thallium plus 426 torr of helium: The solid curves are least-squares fitted. The lower curve is the pure-thallium case.

The effect of rare-gas atoms on the linewidth of the Hanle-effect signals has been previously investigated in a few systems.[22] However, all of these were limited to low metallic densities where only the metal-atom spontaneous emission need be considered. The data taken in our experiment are shown in Fig. 5 along with a least-squares fit to Eq. (5). A least-squares-fitted curve for the pure-thallium case is also presented for comparison at the bottom of the figure. The details of the fitting procedure will be described later.

As expected, the over-all form of the linewidth–vs–thallium-density curve is the same as in the pure-thallium case. Although the general shape is the same, some quantitative differences do exist. (a) The shape and density for the onset of thallium coherence narrowing has changed between the two sets of data, and has shifted toward higher densities where overlapping with resonance-broadening effects becomes more serious. (b) The magnitude of the thallium resonance broadening is reduced in the resonance-broadening region. The above differences imply that (i) the helium-broadening term $N_{He}\sigma_{Tl\text{-}He}\bar{v}_{Tl\text{-}He}$ (here $\sigma_{Tl\text{-}He}$ as defined is $\bar{v}^{-3/5}$ dependent) cannot be simply added to Eq. (4) without any change in the coherence-narrowing and resonance-broadening terms, and (ii) the presence of helium atoms affects the two phenomena. The details of the effect will be discussed in Sec. V.

From Fig. 5, when the thallium densities are very low, the linewidths approach a limiting value. Evidently, in this region only the thallium spontaneous emission and the rare-gas (helium) nonresonance broadening (depolarization) contribute to

the linewidth. From the value of this limiting total linewidth and the natural linewidth obtained in Sec. III, the amount of helium-gas broadening is obtained. From this information the broadening or depolarization cross section is calculated to be

$$\sigma_{T1\text{-}He} = 7\times10^{-13}/\bar{v}\ \text{cm}^2 ,$$

or at 350 °C,

$$\sigma_{T1\text{-}He} = 4\times10^{-18}\ \text{cm}^2 .$$

The accuracy of this cross section is estimated to be no better than 30% because in the determination of $\sigma_{T1\text{-}He}$ the excited-state linewidth for thallium must be subtracted from the over-all thallium-plus-helium linewidth.

When the coherence-narrowing region is approached, the linewidths no longer simply display a constant amount of rare-gas (helium) broadening. The following equation is used to represent the over-all linewidth:

$$\Gamma = \Gamma_0 - \textstyle\sum_i \alpha_i x_i \mathcal{B}_i \Gamma_0 + N_{T1}\sigma_{T1\text{-}T1}\bar{v}_{T1\text{-}T1} + N_{He}\sigma_{T1\text{-}He}\bar{v}_{T1\text{-}He} , \quad (5)$$

where the four terms represent the spontaneous emission, coherence narrowing, resonance broadening, and helium broadening, respectively. The value of the fourth term was obtained in the last paragraph, and the value of Γ_0 obtained from the pure-thallium–case experiments can be safely used here. However, the value of the branching ratio $\mathcal{B}_i$ and the value of the thallium resonance-broadening cross section $\sigma_{T1\text{-}T1}$ should be redetermined by least-squares fitting to account for the effect of rare-gas atoms. Unfortunately, a number of effects complicate the analysis. The introduction of helium serves to at least partially eliminate wall collisions that previously were assumed to maintain thermal equilibrium between $6\,^2P_{3/2}$ and $6\,^2P_{1/2}$. It is reasonable to assume a buildup of the metastable $6\,^2P_{3/2}$ state. If we take this as an optical pumping process, the following equation is obtained[18]:

$$\frac{N_B}{N_A} = \frac{T}{\tau_p} = \frac{\sigma_0 I_0}{W_2 + W_3} ; \quad (6)$$

$$N_A + N_B = N_{T1} , \qquad W_2 = N_A\sigma_{A\text{-}B}\bar{v}_{T1\text{-}T1} ,$$

$$W_3 = N_{He}\sigma_{B\text{-}He}\bar{v}_{T1\text{-}He} ,$$

where subscripts B and A refer to the $^2P_{3/2}$ and $6\,^2P_{1/2}$ states, respectively, T is the relaxation time of the B state, τ_p is the optical pumping time, N is the density, σ_0 is the absorption cross section for thallium 3776-Å photons, I_0 is the incident light intensity, W_2 is the relaxation rate resulting from collisions with ground-state thallium atoms, and W_3 is the relaxation rate resulting from collisions with helium-gas atoms. Here, we neglect the wall relaxation rate in the presence of helium atoms because it is very small compared to W_2 and W_3.[23]

Recently, Pickett and Anderson[24] have measured the cross section $\sigma_{A\text{-}B}$ to be 5.4×10^{-16} cm^2. From this, the value of W_2 can be calculated. Unfortunately, the value of $\sigma_{B\text{-}He}$ is not well known,[25] so we take it as a variable parameter in the fitting. The light intensity I_0 is known and σ_0 is calculable. Thus, Eq. (6) requires only one parameter and from this equation, the densities N_B and N_A can be expressed in terms of this parameter. Accordingly, the total amount of thallium coherence narrowing contributed by N_A and N_B is a function of this parameter along with the parameter for the branching ratio. Therefore, we substitute Eq. (6) into Eq. (5) and use Eq. (5) to least-squares fit the data. Three variable parameters were assigned in the fitting. They correspond to (a) the relaxation cross section of $6\,^2P_{3/2}$ thallium to $6\,^2P_{1/2}$ thallium by helium atoms, $\sigma_{B\text{-}He}$, (b) the branching ratio to the $F=0$ level of the ground state, and (c) the thallium resonance-broadening cross section $\sigma_{T1\text{-}T1}$.

From Eq. (6), the relation between N_B and N_{T1} can be further discussed. For thallium densities $<10^{14}$ atoms/cm^3, $W_3 \gg W_2$ and W_2 can be neglected. Thus,

$$\frac{N_B}{N_A} = \frac{C}{N_{He}\sigma_{B\text{-}He}\bar{v}_{T1\text{-}He}} ,$$

where $C = \sigma_0 I_0$. Since the right-hand side of the above equation is approximately constant, the ratio of N_B/N_A will remain constant ($\sim 10^{-2}$), and N_B, the metastable-state concentration, will increase linearly with an increase in the total thallium concentration. But, when $N_{T1} \gg 10^{14}$ atoms/cm^3, W_2 dominates the relaxation process, W_3 can be neglected, and

$$\frac{N_B}{N_A} = \frac{C}{N_A\sigma_{A\text{-}B}\bar{v}_{T1\text{-}T1}}$$

is obtained. Since N_A cancels and the rest of the terms on the right-hand side of the above equation remain about constant, the value of N_B will thus remain constant in spite of a further increase in the total thallium density. The results of the least-squares fit show this limiting value of N_B to be $\sim 10^{12}$ atoms/cm^3. This density is high enough to cause a significant amount of thallium coherence narrowing, but fortunately is not high enough to completely depolarize the cross-fluorescence light.

The numerical least-squares fit results are shown in Fig. 5. The least-squares-fitted curve fits the experimental data very well, indicating a reasonable data analysis. These results give the relaxation cross section of $6\,^2P_{3/2}$-state thallium to $6\,^2P_{1/2}$-state thallium by helium atoms,

$$\sigma_{B\text{-}He} = \sigma_{T1(6\,^2P_{3/2})\text{-}He} \cong 1\times10^{-21}\ \text{cm}^2 .$$

This value seems very reasonable considering that the separation between the two fine-structure states

is very large (7793 cm^{-1}). The least-squares fit also gives

$$\mathfrak{B}_1 = 1.69\times10^7/\Gamma_0 .$$

This corresponds to a branching ratio to the thallium $6\,^2P_{1/2}$ state of 39%, a value about 10% smaller than the pure-thallium value. The data taken in the broadening region are plotted in Fig. 6. The slope gives a resonance-collision cross section

$$\sigma_{Tl\text{-}Tl} = 4.04\ (0.08)\times10^{-8}/\bar{v}\ cm^2 ,$$

which is smaller than the pure-thallium value by 24%, and differs by about 9 rms standard deviations from the pure-thallium experiments. The error does not include the estimated 6% uncertainty in the density calculation, because we only intend to show the *relative* decrease in the slope from the pure-thallium case.

Loss of rare-gas atoms from diffusion through the cell walls also leads to an apparent relative decrease in $\sigma_{Tl\text{-}He}\,\bar{v}_{Tl\text{-}He}$. The previously mentioned experiment using 113 torr of He gave $\sigma_{Tl\text{-}Tl} = 5.22(0.13)\times10^{-8}/\bar{v}\ cm^2$, which is also smaller than for the pure-thallium case. From an expression given by Dushman[26] and using the diffusion data given by Norton,[27] we estimate the total amount of helium lost during the experiment to be only 4%. This 4% loss of helium will cause only about a 1% decrease in the slope of Γ vs N_{Tl} and we consider the helium diffusion to be unimportant.

We must also assume that wall-broadening effects are negligible. Since the optical depth [optical depth = absorption depth^{-1} × cell length = $(\lambda^2/2\pi)Nx$] for the 3776-Å radiation is about 5.7×10^4 for $N_{Tl}(^2P_{1/2})$ = 10^{14} atoms/cm^3 and about 5.7×10^2 for the 5350-Å transition under the optical pumping conditions, there will be some wall contribution to the linewidth. In the experimental arrangement the exciting and detected light are constrained along the cylindrical-cell axis thus minimizing properties depending on radiation transport. We believe that the wall contribution is small. Another aspect of this radiation transport would be a linewidth dependence on thallium-atom density. As the thallium density is increased the optical depth increases (absorption depth decreases) and wall effects become more and more important. The introduction of helium might then be thought to impede the wall effect thus leading to a relative narrowing of the linewidth. This should lead, however, to an N_{Tl}^2 dependence of the linewidth and such is not observed. In any event we believe the effect to be too small to be of significance. The reduction in the branching ratio on introduction of He is not understood. It may be due to a breakdown in the coherence-narrowing theory as applied to this particular experiment. For example, higher He densities may cause a homogeneous broadening of the Tl line slightly greater than the Doppler width of the lamp thus causing a reduction in absorption and an apparent change in the branching ratio.

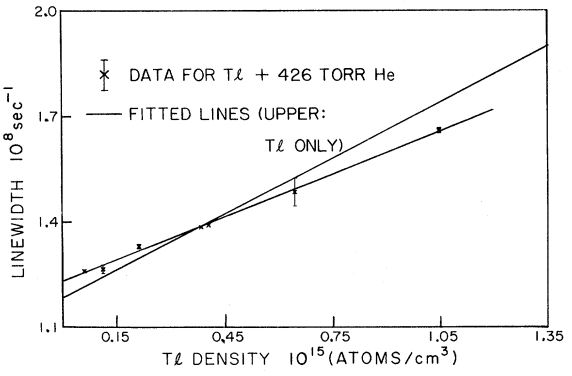

FIG. 6. Data for thallium plus 426 torr of helium: Linewidth vs thallium density in the broadening region.

The relative decrease in linewidth (lowering of the slope of the Γ-vs-N_{Tl} curve at high densities) with the addition of a foreign gas cannot be explained solely on the basis of two-body collisions. This makes physical sense since the helium density is high, 2×10^{19} atoms/cm^3. The concomitant distortion of the thallium wave function under helium collisions means that a collision between this "complex" and another thallium atom will no longer be so sharply resonant.

Experiments were also performed using argon as the buffer gas. The collisional-depolarization cross section for thallium-argon collisions was found to be

$$\sigma_{Tl\text{-}Ar} = \begin{cases} 8\times10^{-13}/\bar{v}\ cm \\ 1\times10^{-17}\ cm^2 \text{ at } 350\,^\circ C. \end{cases}$$

V. SUMMARY OF RESULTS

The experimental results are summarized in Table I. In the case of pure thallium, the value of the thallium $7\,^2S_{1/2}$-state lifetime agrees well with the results obtained by Gallagher and Lurio[7] and Norton and Gallagher.[21] The branching ratio is found to disagree with the branching ratio determined by Gallagher and Lurio and probably reflects inaccuracies in the theory for radiation trapping as applied to this experiment. The resonance-broadening cross section also differs from theory. This is due to the inapplicability of resonance-broadening theory to the specific case of $7\,^2S_{1/2}$ thallium as discussed in the following paper by Omont, and the present authors.

Data obtained from the experiment containing 426 torr of helium in addition to thallium show that helium-gas-atom collisions alter the thallium coherence narrowing and decrease the degree of thallium resonance broadening. Detailed analysis of

TABLE I. Summary of results.

Item	Pure-thallium case	Thallium + 426 torr of He
τ_0 [a]	7.55 (0.08) × 10^{-9} sec	
Branching ratio to the ground state	43%	39%
$\sigma_{Tl\text{-}Tl}$ [b]	$5.38\times10^{-8}/\bar{v}$ cm^2	$4.04\times10^{-8}/\bar{v}$ cm^2
$\sigma_{Tl(6^2P_{3/2})\text{-}He}$ [c]		1×10^{-21} cm^2
$\sigma_{Tl\text{-}He}$ [d]		$7\times10^{-13}/\bar{v}$ cm^2 4×10^{-18} cm^2 [e]

[a]The natural lifetime of the thallium 7S state.

[b]The thallium-thallium resonance-broadening cross section.

[c]The relaxation cross section of $6\,^2P_{3/2}$-state thallium to $6\,^2P_{1/2}$-state thallium by helium atoms.

[d]The 7^2S thallium-helium atom broadening, or depolarization cross section.

[e]At 700 °C.

the data, using Eq. (5), shows that the buildup of the thallium metastable-state concentration, which introduces another contribution to the coherence narrowing, can well explain the change of the thallium coherence narrowing by the addition of helium. The analysis also produced the result that the branching ratio to the ground state decreased 10% from the pure-thallium case (from 43 to 39%), the thallium resonance-broadening cross section decreased 24% (from $5.38\times10^{-8}/\bar{v}$ to $4.04\times10^{-8}/\bar{v}$ cm^2), and an estimate of the relaxation cross section of the $6\,^2P_{3/2}$ state to the $6\,^2P_{1/2}$ state in thallium by helium atoms of 10^{-21} cm^2 is also obtained. The lowering of the branching ratio is not understood, but may have to do with helium pressure broadening of the thallium transition. One would not expect collisions with helium to alter the thallium wave function significantly enough to change the transition probability to such an amount. On the other hand, it is reasonable to expect helium-thallium collisions to alter the energy levels of thallium enough so that the Tl*-Tl collisions become somewhat nonresonant. The 24% decrease in the resonance-broadening cross section indicates the influence of three-body collisions, between thallium and helium atoms, on the linewidth. Similar results were obtained with 419 torr of argon. The effects of three-body collisions is discussed in the following paper by Omont *et al.*

ACKNOWLEDGMENTS

One of the authors (J. C. B.) would like to thank Dr. A. V. Phelps, of JILA, for many illuminating discussions about radiation transport, Professor K.-I. Gondaira, University of Electrocommunications, Tokyo, for insights into coherence-narrowing phenomena, and Professor A. Omont, Laboratoire de Spectroscopie Hertzienne de l'ENS Faculte des Sciences, Paris, and a Visiting Fellow at JILA, for many helpful comments about the experiment.

APPENDIX

The theoretical expression for the signal will be derived here along with a demonstration of selection rules.

The Breit equation[4] can be expressed by

$$R\propto\sum_{b,b'}\sum_{a,a'}\frac{\langle b'|H_2|a\rangle\langle a|H_2|b\rangle\langle b|H_1|a'\rangle\langle a'|H_1|b'\rangle}{1-2\pi i\tau\nu(b',b)}\,, \tag{A1}$$

where H_1 and H_2 are the electric-dipole-transition Hamiltonian for the annihilation of the incident photons and for the creation of the outgoing photon, respectively; R is the radiation rate; τ is the mean lifetime of the excited sublevels $|b\rangle$ and $|b'\rangle$; $\nu(b',b)=(E_{b'}-E_b)/\hbar$ is the frequency separation between the excited sublevels. For a zero-field level-crossing experiment, $|J,\ F,\ M_F\rangle$ are appropriate basis states with which to construct $|b\rangle$, $|b'\rangle$. We write

$$|b\rangle=\sum_{J,F}|JF\mu\rangle\langle JF\mu|U|b\rangle\,, \tag{A2}$$

where μ is the equivalent to M_F. Substituting (A2) into (A1), and following Rose and Carovillano's procedure, we obtain

$$S\propto\sum_{b,b'}\sum_{\substack{J,F,\bar{J},\bar{F}\\ J'F',\bar{J}',\bar{F}'}}\frac{\langle JF\mu|U|b\rangle\langle\bar{J}\,\bar{F}\mu|U|b\rangle^*\langle\bar{J}'\bar{F}'\mu'|U|b'\rangle\langle J'F'\mu'|U|b'\rangle^*}{1-2\pi i\tau\nu(\mu',\ \mu)}$$

$$\times\langle\bar{J}\bar{F}\mu|M_1|\bar{J}'\bar{F}'\mu'\rangle\langle JF\mu|M_2|J'F'\mu'\rangle^*\,, \tag{A3}$$

where

$$\langle\bar{J}\bar{F}\mu|M_1|\bar{J}'\bar{F}'\mu'\rangle=\sum_{F_1,m_{F_1}}\langle\bar{J}\,\bar{F}\mu|M_1|J_1F_1m_{F_1}\rangle\langle J_1F_1m_{F_1}|H_1|J_1F'\mu'\rangle$$

and the M_2 matrix has a similar expression. For dipole radiation we obtain

$$\langle\bar{J}\,\bar{F}\mu|M_1|\bar{J}'\bar{F}'\mu'\rangle=(-)^{J_1-I+\mu-1}[(2\bar{J}+1)(2\bar{J}'+1)(2\bar{F}+1)(2\bar{F}'+1)]^{1/2}\langle\bar{J}\,||1||\bar{J}_1\rangle\langle\bar{J}'||1||\bar{J}_1\rangle^*\sum_{\nu}(2\nu+1)$$

$$\times \begin{Bmatrix} \bar{J}_1 & \bar{J} & \nu \\ \bar{F} & \bar{F}' & I \end{Bmatrix} \begin{Bmatrix} 1 & 1 & \nu \\ \bar{J}' & \bar{J} & J_1 \end{Bmatrix} \begin{pmatrix} 1 & 1 & \nu \\ P & -P & 0 \end{pmatrix} \begin{pmatrix} \bar{F} & \bar{F}' & \nu \\ -\mu & \mu' & \mu-\mu' \end{pmatrix} D^{\nu}_{\mu-\mu',0}(\phi_1, \theta_1, 0) , \quad \text{(A4)}$$

where θ_1 and ϕ_1 denote the polar angles of the direction of the incident light, and $D^{\nu}_{\mu-\mu',0}$ is an element of the rotation matrix. The expression for the M_2 matrix element can be obtained by replacing θ_1, ϕ_1 with θ_2, ϕ_2 and by an appropriate change of quantum numbers.

Now, the complete selection rules can be deduced from Eq. (A4). From the properties of the 6-j and 3-j symbols, one easily notices that the following relations should hold simultaneously in order to have a coherent signal:

$$0 \leq \nu \leq 2 \quad \text{and} \quad 0 \leq |\mu - \mu'| \leq 2 .$$

In this work, $J_1 = \frac{1}{2}$, $I = \frac{1}{2}$, $F_1 = 0$, 1; $\bar{J} = \bar{J}' = \frac{1}{2}$; and $\bar{F}$, $\bar{F}' = 0$, 1.

(i) $|\mu - \mu'| = 0$. This is an anticrossing case requiring $\bar{F} = \bar{F}'$. In the thallium $7\,^2S_{1/2}$ state, only the $F = 0$ and $F = 1$, $M_F = 0$ sublevels, which satisfy this case, may contribute an anticrossing signal. However, since the 12000-MHz separation of the two hfs components is far larger than the 132-MHz natural linewidth, and there is also the 2000-MHz Doppler width, no anticrossing signal can be detected.

(ii) $|\mu - \mu'| = 2$. In this case, $\nu = 2$ must be satisfied. But $\bar{J} = \frac{1}{2}$, $\bar{J}' = \frac{1}{2}$, and $\nu = 2$ cannot form a triangle relation in the two 6-j symbols of Eq. (A4), thus, there can be no $\nu = 2$ coherent signal. Since $\nu = 2$ corresponds to either a linear or unpolarized light, no level-crossing signal can be detected from an excited state with $J = \frac{1}{2}$ by employing either linear or unpolarized incident light.

(iii) $|\mu - \mu'| = 1$. In this case, $\nu = 1$ or 2, but $\nu = 2$ is not allowed as just stated. $\nu = 1$ satisfies a triangle relation with values of $\bar{J}'$ and $\bar{J}$.

Consequently, these selection rules imply that for a $J = \frac{1}{2}$ excited state, only the $\nu = 1$ level-crossing signal can be observed. Thus, one has to use circular-polarized exciting light and also detect the circular-polarized scattered light. Furthermore, since in the first 6-j symbol of Eq. (A4), $\bar{J}$, $\bar{J}'$, ν and $\bar{F}$, $\bar{F}$, ν must maintain triangle relations simultaneously, it is obvious that when $\bar{F} = \bar{F}' = \frac{1}{2}$, the same selection rules as just described for $\bar{J}, \bar{J}' = \frac{1}{2}$ will hold. For example, in the $6P_1$ state of ^{199}Hg, where $J = 1$, there is still no $\nu = 2$ level-crossing signal occurring from the $F = \frac{1}{2}$ level. A part of these selection rules were also deduced by Gallagher and Lurio[7,28] through a different procedure.

For $|\mu - \mu'| = 1$ and $\nu = 1$, the geometrical dependents of the signal is determined by the element of the rotation matrix:

$$D^1_{\pm 1,0}(\phi_1, \theta_1, 0) = -(\tfrac{4}{3}\pi)^{1/2} Y_{1,\pm 1}(\theta_1, \phi_1)$$
$$= \pm (\tfrac{1}{2})^{1/2} \sin\theta_1 e^{\pm i\phi_1} . \quad \text{(A5)}$$

If 5350-Å cross-fluorescence light is to be detected, we use Eq. (A5) in the M_1 and M_2 matrix elements, and then substitute into Eq. (A3). We finally arrive at the following expression for the detected signal strength:

$$S = A - B \frac{(\pm)(\pm)\sin\theta_1 \sin\theta_2}{1 + (E_{\mu,\mu'}\tau)^2}$$
$$\times [\cos(\phi_1 - \phi_2) + E_{\mu,\mu'}\tau \sin(\phi_1 - \phi_2)] . \quad \text{(A6)}$$

There are two ways in which this equation differs from Eq. (13) of Ref. 7, which was derived by assuming detection of 3776-Å scattered light. (a) The sign of the coherent part of the signal is reversed. This fact comes from the phase factor in the M_2 matrix element, namely,

$$(-1)^{J_2 - I + \mu - 1} ,$$

where $J_2 = \frac{1}{2}$ (3776-Å light detected) the sign is just the reverse of the $J_2 = \frac{3}{2}$ case (5350-Å light detected). (b) The magnitude of the coherent signal β is about one-half that in Ref. 7. This fact comes from the second 6-j symbol of the M_2 matrix element [cf. Eq. (A4)] which is the only J_2-dependent term.

*Supported in part by the National Science Foundation under Grant No. GP-8984, and in part by the Petroleum Research Fund under Grant No. 3205-A5.

†Present address: Radiation Laboratory, Notre Dame University, Notre Dame, Ind. 46556.

‡Visiting Fellow, on leave from Brown University.

[1]W. Gough and G. W. Series, Proc. Phys. Soc. (London) 85, 467 (1965); K. C. Brog, T. G. Eck, and H. Wieder, Phys. Rev. 153, 91 (1967); M. W. Swagel and A. Lurio, *ibid.* 169, 114 (1968).

[2]E. B. Saloman and W. Happer, Phys. Rev. 144, 7 (1966).

[3]W. Happer and E. B. Saloman, Phys. Rev. 160, 23 (1967).

[4]G. Breit, Rev. Mod. Phys. 5, 91 (1933).

[5]P. A. Franken, Phys. Rev. 121, 508 (1961).

[6]M. E. Rose and R. L. Carovillano, Phys. Rev. 122, 1185 (1961).

[7]A. Gallagher and A. Lurio, Phys. Rev. 136, A87 (1964).

[8]M. W. Zemansky, Phys. Rev. 29, 513 (1927).

[9]J. P. Barrat, J. Phys. Radium 20, 541 (1959).

[10]J. P. Barrat, J. Phys. Radium 20, 633 (1959); see also Ref. 9.

[11]M. I. D'yakonov and Y. I. Perel, Zh. Eksperim. i Teor. Fiz. 47, 1483 (1964) [Sov. Phys. JETP 20, 997

(1965)].
[12]F. W. Byron, Jr. and H. M. Foley, Phys. Rev. 134, A625 (1964).
[13]A. Omont, Ph.D. thesis (University of Paris, 1967) (unpublished); A. Omont, J. Phys. (Paris) 26, 26 (1965); A. Omont and J. Meunier, Phys. Rev. 169, 92 (1968).
[14]M. I. D'yakonov and V. I. Perel', Zh. Eksperim. i Teor. Fiz. 48, 345 (1965) [Sov. Phys. JETP 21, 227 (1965)].
[15]P. R. Berman and W. E. Lamb, Jr., Phys. Rev. 187, 221 (1969).
[16]From alloy data published by the Omega Engineering Inc., Springdale, Conn.
[17]L. K. Genov, A. N. Nesmeyanov, and T. A. Priselkov, Dokl. Akad. Nauk SSSR 140, 159 (1961) [Sov. Phys. Doklady 140, 670 (1961)]; A. N. Nesmeyanov, *Vapor Pressure of the Elements*, translated by J. I. Carasso (Academic, New York, 1962).
[18]C.-C. Hsieh, Ph. D. thesis (Brown University, 1970) (unpublished); C. C. Hsieh and J. C. Baird, J. Chem. Phys. 53, 3378 (1970).
[19]R. E. Honig, RCA Rev. 23, 567 (1962).
[20]W. E. Wentworth, J. Chem. Educ. 42, 96 (1965).
[21]M. Norton and A. Gallagher, Phys. Rev. A 3, 915 (1971).
[22]A. Gallagher, Phys. Rev. 157, 68 (1967); S. Teplova, M. Chaika, and V. Cherenkovskii, Opt. i Spektroskopiya 25, 346 (1968) [Opt. Spectry. (USSR) 25, 189 (1968)].
[23]See W. Franzen, Phys. Rev. 115, 850 (1959); R. A. Bernheim, J. Chem. Phys. 36, 135 (1962).
[24]R. C. Pickett and R. Anderson, J. Quant. Spectry. Radiative Transfer 9, 697 (1969).
[25]J. A. Bellisio and P. Davidovits, J. Chem. Phys. 53, 3474 (1970).
[26]S. Dushman, *Scientific Foundations of Vacuum Technique* (Wiley, New York, 1962), Chap. 7.
[27]F. J. Norton, J. Am. Ceram. Soc. 36, 90 (1953).
[28]A. Gallagher and A. Lurio, Phys. Rev. Letters 10, 25 (1963).

PHYSICAL REVIEW A VOLUME 6, NUMBER 1 JULY 1972

Level-Crossing Spectroscopy in $7\,^2S_{1/2}$ Thallium. II. Theory of Self-Broadening and Tl*-Tl–Foreign-Gas Collisions

A. Omont*
Joint Institute for Laboratory Astrophysics, University of Colorado, Boulder, Colorado 80302

and

J. C. Hsieh
The Radiation Laboratory, University of Notre Dame, Indiana 46556

and

J. C. Baird†
Joint Institute for Laboratory Astrophysics, University of Colorado, Boulder, Colorado 80302

(Received 23 August 1971)

The experimental results for the self-broadening of pure Tl of the previous paper are shown to be in good agreement with the theory of resonant collisions, taking into account the effects of the hyperfine structure. Wall collisions are nearly negligible in that case. The decrease of the self-broadening observed with the addition of a foreign gas is explained in terms of three-body collisions (Tl-He collisions occurring during a Tl*-Tl collision) which broaden the optical transitions of Tl and decrease the resonance effect in the transfer of excitation between Tl atoms. The quantitative agreement obtained with the experimental results shows that these three-body collisions must be responsible for the major part of the observed reduction in self-broadening.

I. INTRODUCTION

In the previous paper[1] on zero-field level crossing in atomic thallium (Hanle effect) several observations were made. Among these were (a) the resonance-broadening cross section for thallium-thallium excitation-transfer collisions and (b) the fact that in the presence of a foreign gas, either helium or argon, the resonance-broadening cross section was reduced. In the first case, agreement with theory was less than expected and in the second case there existed no suitable theoretical description. It is the purpose of this paper to present a theoretical explanation of these two effects.

The theories of D'Yakonov and Perel',[2] Byron and Foley,[3] Omont and Meunier,[4] Kazantsev,[5] and Berman and Lamb[6] on resonance-broadening line shapes are based on several assumptions among